The dual nature of the martian crust: Young lavas and old clastic materials

Joshua L. Bandfield [a,*], Christopher S. Edwards [b], David R. Montgomery [a], Brittany D. Brand [a]

[a] Department of Earth and Space Sciences, University of Washington, Seattle, WA 98195-1310, United States
[b] School of Earth and Space Exploration, Arizona State University, Tempe, AZ 85287-6305, United States

A B S T R A C T

Visible and thermal infrared spacecraft datasets are used to gain insight into the nature of the surface materials and upper martian crust, revealing a distinct transition in the physical properties of martian crustal materials that occurred during the Hesperian era. Contrary to a prevailing view of the martian crust as primarily composed of lava flows, we find that most older regions of Mars have morphological and thermophysical properties consistent with poorly consolidated fine-particulate materials that may have a volcaniclastic origin. By contrast, younger surfaces contain blocky materials and thermophysical properties consistent with effusive lava flows. Explosive volcanism is likely to have been dominant on early Mars and these findings have implications for the evolution of the volatile content of the crust and mantle and subsequent development of the surface morphology. This dual nature of the crust appears to be a defining characteristic of martian history.

© 2012 Elsevier Inc. All rights reserved.

1. Introduction

A prevalent view of the upper martian crust is that it is dominantly composed of lava flows that may have been subsequently disrupted by the creation of a mega-regolith through impact events. Previous studies have established that the martian upper crust is mechanically weak (e.g., Pike, 1980; Schultz, 2002; Stewart and Valiant, 2006) and the notion of a mega-regolith that has been highly fractured and disrupted similar to that of the Moon has typically been invoked as the cause of this weakness. However, extensive exposures of layered materials are present that have been attributed to the presence of undisrupted lava flows, sediments or volcanic ash (McEwen et al., 1999; Malin and Edgett, 2000; Beyer and McEwen, 2005).

Here we reexamine the notion of a martian crust dominantly composed of effusive lavas (disrupted or otherwise) in light of more recent high resolution visible and thermal infrared observations. We find that, in older Noachian terrains, the upper $\sim$2–10 km of the martian crust (where exposed) is typically weakly consolidated, consistent with previous studies (Pike, 1980; Schultz, 2002; Stewart and Valiant, 2006). However, these crustal materials have morphological and thermophysical properties that are inconsistent with highly fractured, competent blocks (>10s of cm in diameter) such as what may be derived from lava flows or well-cemented sandstones. Rather, the upper martian crust is more typically composed of poorly consolidated, fine-particulate materials

in these regions. Conversely, competent blocky materials appear to be common in younger regions.

The basic processes that form the crust of a planet are a fundamental aspect of planetary development that establishes a basis for shaping more detailed investigations. A goal of this work is to investigate the hypothesis that explosive mafic volcanism was a dominant process early in martian history and was followed by a later period where effusive volcanism was more common (e.g., Reimers and Komar, 1979; Robbins et al., 2011). We propose that the ultimate origin of the fine-particulate crustal materials is explosive volcanism, although subsequent reworking and processing of these volcaniclastic materials (such as in the formation of a mega-regolith) has clearly occurred in many instances.

It is useful to define the terms "volcaniclastic" and "explosive volcanism" as they are used here. "Explosive volcanism" refers to volcanic activity that primarily produces fine-particulate ash rather than high strength blocks or lava flows. The term "volcaniclastic" refers to materials that result from explosive volcanism and the potential reworking of these products by impact, aeolian, or fluvial processes. In addition, we refer to materials as "high strength" or "weakly consolidated" based on interpretations of images and thermal inertia data. High-strength materials are characterized by abundant blocks that persist significant distances from their source and high-thermal inertias (>$\sim$600 J m^{-2} K^{-1} s$^{-1/2}$). Weakly consolidated materials do not form block-dominated surfaces and where blocks are present, they are easily disaggregated over distances of a several hundred meters. Surfaces dominated by these materials are characterized by low thermal inertia values (<$\sim$600 J m^{-2} K^{-1} s$^{-1/2}$).

* Corresponding author.
 E-mail address: joshband@u.washington.edu (J.L. Bandfield).

Extensive layered sequences are present in regions such as the interior of Valles Marineris or Meridiani Planum. There are many geological processes by which layered materials can be produced and the sources of these thick sequences on Mars remains the subject of considerable debate (e.g., Malin and Edgett, 2000; Schultz, 2002; Adams et al., 2009; Jackson et al., 2011). These materials are of considerable interest in their own right and may be considered a significant component of the martian crust, but their origin is not addressed here.

2. Methods and observations

Spacecraft observations provide evidence for weak, poorly cohesive deposits exposed in thick crustal sections within Valles Marineris, craters, and other valleys on Mars. The 2001 Mars Odyssey Thermal Emission Imaging System (THEMIS; Christensen et al., 2004) day and night infrared mosaics provide regional morphological and thermophysical information (Edwards et al., 2011). For local areas of interest, we derived 100 m/pixel thermal inertia maps from individual THEMIS images (Fergason et al., 2006a). These thermal inertia observations are an effective means of determining the particle size and degree of consolidation of exposed materials (e.g., Kieffer et al., 1977; Mellon et al., 2000; Fergason et al., 2006a,b), and are used to distinguish high-strength layers (e.g., lava flows, well-cemented sediments) from fine-grained, poorly cohesive layers (e.g., volcaniclastic or poorly cemented/loose sediments). We did not take local slopes into account because topography data was not available at the spatial resolution of the THEMIS observations. This will introduce some uncertainty in the derived thermal inertia values. For example, a $150 \, \mathrm{J \, m^{-2} \, K^{-1} \, s^{-1/2}}$ surface at 20°N and L_s 0°, 20° north and south facing slopes will result in derived thermal inertia values of 120 and $218 \, \mathrm{J \, m^{-2} \, K^{-1} \, s^{-1/2}}$ respectively if slopes are not taken into account. This range of values would have little effect on the subsequent interpretation for the purpose of our work.

Mars Reconnaissance Orbiter (MRO) Context Camera (CTX; Malin et al., 2007) images (typically ~5.5 m sampling) were used to provide corresponding morphological information. MRO High Resolution Imaging Science Experiment (HiRISE; McEwen et al., 2007) red filter images sampled at 0.25–0.5 m/pixel were used to describe surface textures and morphology and to identify the presence of blocks.

We have organized observations into several basic categories based on geography or type of feature. In some cases, these are the results of previous studies that directly contribute to our thesis and we summarize them here. Our own observations rely primarily on the imaging and thermophysical datasets described above and we show how these data can be used to distinguish competent, high strength materials from mechanically weak, fine-grained materials.

2.1. Valles Marineris

The walls of Valles Marineris expose the martian crust with ~7–10 km of vertical relief running nearly the full length of the canyon system. The wall slopes are shallow (~10–30°; Schultz, 2002), implying a low strength of the material, generally attributed to highly fractured materials (Clow et al., 1988; Schultz, 1991, 1996, 2002; Lucchitta et al., 1992; Caruso and Schultz, 2001; Peulvast, 2001). For example, Schultz (2002) examined slopes of the walls of Valles Marineris and determined cohesion values of ~0.1–0.2 MPa and friction angles of 14–25°. The rock strengths appear vertically and laterally homogeneous and the slopes are not consistent with intact rock, but either a heavily fractured and perhaps altered basalt or a mechanically competent unwelded to welded tuff (Schultz, 2002). Interior deposits have lower slopes and different patterns of thermal inertia, mineralogy, and morphology (i.e., wind eroded, absence of landslides) and are widely regarded as being separate deposits that either postdate valley formation (e.g., Schultz, 2002) or are exhumed from beneath wall rock (e.g., Malin and Edgett, 2000). A more complete analysis of these deposits is beyond the scope of this work, but we note their contrast in properties from the walls.

Thermal inertia values derived from THEMIS nighttime temperature data (Fig. 1) for the majority of the layered crust exposed within the wall rock of the Valles Marineris system are relatively low ($\sim$200–300 $\mathrm{J \, m^{-2} \, K^{-1} \, s^{-1/2}}$). These observations are consistent with poorly consolidated or loose fine-particulate materials and
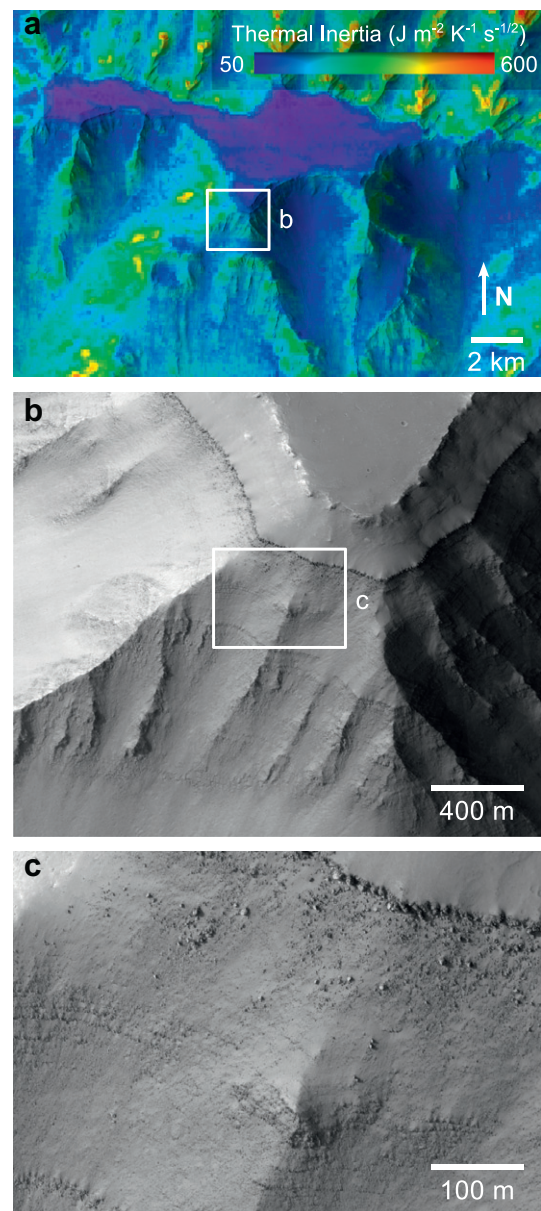

Fig. 1. (a) Surface thermal inertia data within Coprates Chasma (near 304.1E, 14.4S) derived from 100 m/pixel THEMIS data (I19030003) with CTX image B06_01192_1653_XI_14S055W used for shading. Thermal inertia values remain low across the 4.5 km elevation range visible within the image despite the exposure of layering on steep slopes. (b and c) Portion of HiRISE image PSP_002036_1655 displaying layered exposures near the canyon rim. Although boulders are present near the top of the wall, they are not shed from lower layers and do not persist down slope, indicating that they are weakly consolidated and easily disaggregated.

are inconsistent with lava flows or high strength blocks. Assuming loose particulates of uniform size, these values of thermal inertia would be composed of fine sand-sized particles (~150 μm diameter; Presley and Christensen, 1997; Piqueux and Christensen, 2011). The particle sizes can be larger or the materials may be more cohesive if the region is partially mantled by dust. These thermal inertia values are also consistent with finer particulates that are somewhat cohesive.

High-resolution imaging of many low thermal inertia materials exposed within the walls of Valles Marineris show layers that appear variably resistant (Beyer and McEwen, 2005). The majority of the individual layers are laterally continuous, but can also occasionally pinch and swell or be truncated by overlying deposits (Fig. 1). The stratigraphy of the upper several kilometers of the Valles Marineris system dominantly displays repetitive bedding where more resistant layers are separated by 10s of layers of less resistant, thinner layers. The more resistant layers display a rough texture at meter scales and produce boulders; however, the blocks do not persist more than several hundred meters down slope. This observation suggests that the blocks are also composed of weakly consolidated materials that disaggregate under minimal downslope transport (Malin and Edgett, 2000).

Although these examples typify the wall materials exposed throughout the Valles Marineris system, not all exposures are finely layered. Much of the lower extent of the walls appears covered with debris and they are highly disrupted. However, where exposures are present, thermal inertia values are still typically much lower than that of block-dominated surfaces, and boulders are not common in HiRISE images.

High thermal inertia, blocky, olivine-rich basalts are present within Valles Marineris and are exposed in a laterally extensive layer typically less than 500 m in thickness near the base of the canyon system (Fig. 2; Edwards et al., 2008). The layers within this cliff-forming unit can have thermal inertia values >1200 J m^{-2}-K^{-1} s$^{-1/2}$ and are not separated by multiple thinner, less resistant layers as observed at higher elevations within the canyon. Rather they are thick and laterally continuous to sinuous, and produce abundant boulders that collect at the base of the scarp ~1000 m lower in elevation (Fig. 2).

This high thermal inertia material predates the superposed canyon walls sequence and is not stratigraphically extensive. This unit is not likely to be an intrusive sill based on its sheer lateral and limited vertical extents and lack of any confining layers of sufficient mechanical strength. These high-strength materials are consistent with effusive volcanism and are easily distinguished from fine particulates and weakly consolidated layers.

2.2. Other channels and plains surfaces

Other regions of exposed crustal materials, such as outflow channels, can also be used to provide insight to the physical nature of the upper martian crust. High-strength, blocky materials are typically absent from the ~1 to 2.5 km vertical extent of the valley walls, such as in Ares Valles, Ganges Chasma, and Kasei Valles (Fig. 3). However, it is common for laterally extensive exposures of high thermal inertia materials to be present on the valley floors, which may be indicative of a high-strength layer that exerts a control on depth of incision. In the case of Ares Valles, a 1000 km stretch of the valley floor has exposures of elevated thermal inertia materials that are confined to a 200 m range of elevations (Fig. 3). These high thermal inertia materials (575–840 J m^{-2} K^{-1} s$^{-1/2}$) have been previously noted and mapped by Rogers et al. (2005). As shown in Fig. 3, the plains outside of Ares Valles also exhibit extensive elevated thermal inertia materials (500–550 J m^{-2} K^{-1}-s$^{-1/2}$; Rogers et al., 2005) that fall within a 200 m elevation range separate from that exposed on the floor of Ares Valles. It appears
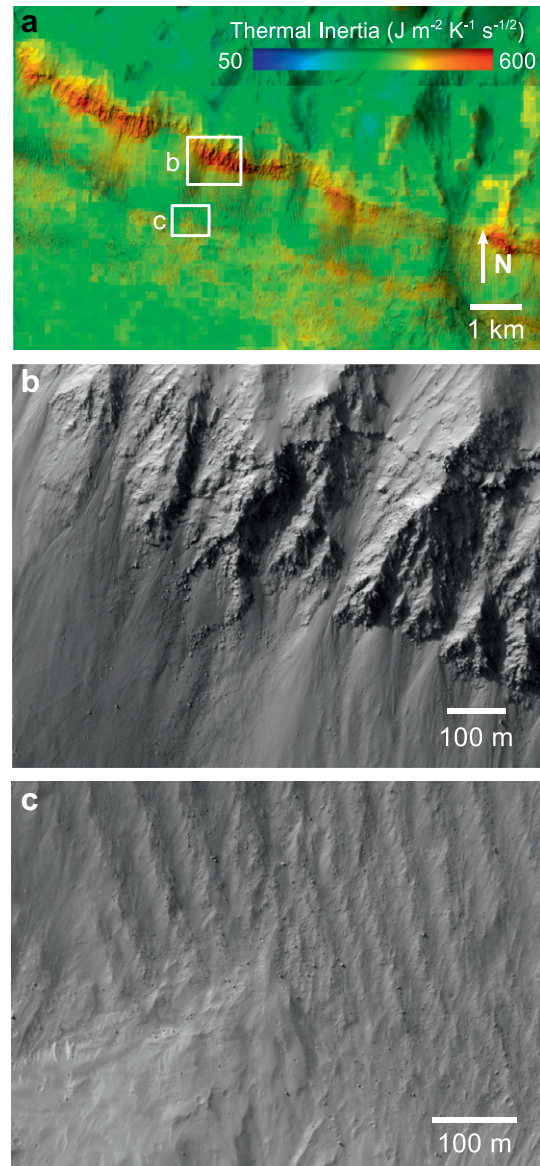

Fig. 2. (a) Surface thermal inertia data near the base of Coprates Chasma (near 293.8E, 11.4S) derived from 100 m/pixel THEMIS data (I18319006) with CTX image P16_07258_1686_XN_11S066W used for shading. Regions of high thermal inertia (orange and red) are similar to an extensive olivine-rich basalt layer documented by Edwards et al. (2008). (b and c) Portions of HiRISE image PSP_008695_1600 displaying layered exposures near the base of the canyon. (b) Displays the high thermal inertia layer and (c) displays boulders that have traveled 1–2 km from the high thermal inertia unit to the base of the canyon wall. The high thermal inertia values and the persistence of boulders with transport indicate that they are composed of well-consolidated and relatively high strength materials. (For interpretation of the references to color in this figure legend, the reader is referred to the web version of this article.)

that stratigraphically thin, high strength units near −2100 and −3800 m elevations in this region sandwich more extensive poorly cohesive materials. Once the upper unit is breached in an outflow event, the surface would be rapidly downcut to the next resistant layer.

The floor of Kasei Valles also contains high thermal inertia materials primarily confined to the valley floor, though the floor slopes significantly to the east away from Tharsis and the layer is not confined to a narrow range of elevation. In both Ares Vallis and Kasei Vallis, the ~1–2.5 km vertical extent of the valley walls typically lack high thermal inertia materials that would indicate the presence of high strength blocky materials.
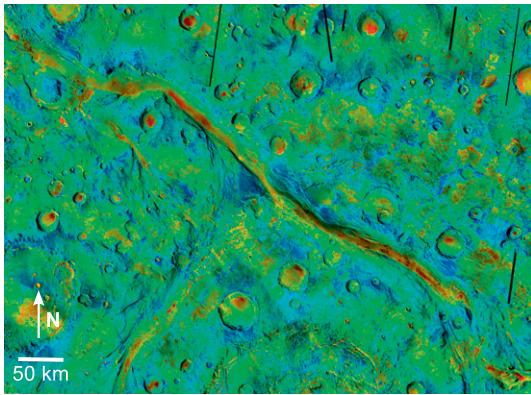
Fig. 3. THEMIS nighttime band 9 radiance global mosaic (color) overlaid on THEMIS daytime band 9 radiance global mosaic (shading). Ares Valles runs from the southeast to the northwest and the image is centered near 338E, 8N. Regional nighttime radiance variations are dominated by thermal inertia and higher values (orange and red) indicate the presence of higher thermal inertia materials. The floor of the channel remains relatively constant throughout the image and is dominated by high thermal inertia materials. An additional high inertia unit is located to the northeast ∼1.5 km above the channel floor. (For interpretation of the references to color in this figure legend, the reader is referred to the web version of this article.)

The flood deposits may consist of cobbles and gravel on the channel floors and the floors might not reflect the thermophysical properties of the local bedrock. This is not likely to be the case for several reasons, however. First, cobble dominated surfaces would not show significant fracturing as can be seen in the floor of some of the channels, such as Ares Valles. In addition, this scenario would require a narrow size distribution that restricts clast sizes to less than can be observed in HiRISE images (<∼1 m). Although it may be possible for the flood events to have restricted the clast size distribution, this is unlikely to have occurred over the great lengths of the channels. Finally, because the low inertia walls of the channels are not a significant source of cobbles, any cobbles present must have been transported from upstream if they are not derived from the floor itself. It is unlikely that they would survive transport of hundreds of kilometers without significant modification and mixing from other sources that would be apparent with thermophysical and morphological measurements along the channel.

2.3. Craters

Craters within the southern highlands also display distinctive thermophysical properties consistent with low strength and poorly consolidated fine particulates (Fig. 4). The walls of these craters commonly have ∼2 km of relief between the floor and rim and often display heavily degraded and disrupted layering with values of thermal inertia typically less than 300 J m^{-2} K^{-1} s$^{-1/2}$. These walls often appear to be easily eroded and mantled with locally derived material. The adjacent floors of craters within many regions of the southern highlands display elevated values of thermal inertia that commonly exceed 600 J m^{-2} K^{-1} s$^{-1/2}$ (Edwards et al., 2009; Fig. 5) and highly fractured surfaces consistent with high-strength rock exposures (Fig. 4). These floor surfaces are possibly derived from post-impact volcanism and show a clear contrast to the adjacent crater walls.

The bulk of the extensively exposed crust within these regions show what appears to be low thermal inertia (typically less than 300 J m^{-2} K^{-1} s$^{-1/2}$ and rarely exceeding 600 J m^{-2} K^{-1} s$^{-1/2}$), weakly consolidated materials that are sometimes finely layered. Although mass wasting may produce identifiable boulders, these boulders are only present in limited pockets and do not survive
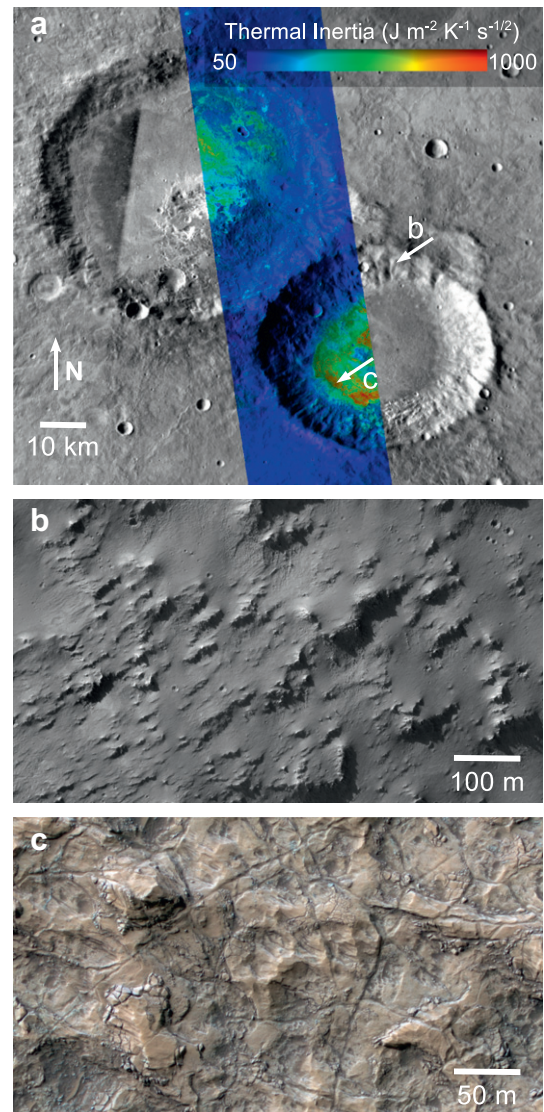

Fig. 4. (a) THEMIS-derived thermal inertia overlain on the daytime band 9 radiance global mosaic in the Terra Sabaea region (near 46.5E, 25.0S). High thermal inertia materials are located within crater floors but are largely absent from the crater rims. This pattern is typical of many craters within the southern highlands. The white arrows denote the locations of high resolution images shown in (b and c). (b) HiRISE image PSP_009126_1545 displays crater wall materials that are typically dominated by low thermal inertia materials and are lacking significant fractures, rocks, or other features that would indicate the presence of high-strength materials. (c) HiRISE image PSP_007689_1540 displays highly fractured blocky materials and is coincident with the high thermal inertia region shown in (a).

transport over significant distances. The presence of a mega-regolith that is largely composed of highly-fractured, high-strength blocks appears to be contradicted by (1) the relatively low thermal inertia values of the exposed stratigraphy, (2) the presence of laterally extensive, mechanically competent rock units that occur both stratigraphically above and below lower thermal inertia exposures, and (3) in some areas, the continuous fine-scale layering that is present.

Crater morphology also lends insight into the mechanical strength of the crust. For example, crater depth to diameter ratios and complex crater onset diameters are typically consistent with a mechanically weak martian crust (Pike, 1980; Stewart and Valiant, 2006; Boyce et al., 2006). Isidis Planitia and Utopia Planitia have been identified as regional exceptions to this trend with depth to diameter ratios that indicate the presence of a high strength target
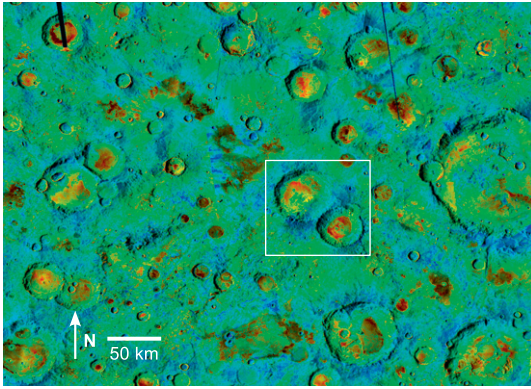
Fig. 5. THEMIS nighttime band 9 radiance global mosaic (color) overlaid on THEMIS daytime band 9 radiance global mosaic (shading). The image covers Terra Sabaea and is centered near 45E, 24S. High thermal inertia units are located within crater floors as well as within a limited elevation range on the inter-crater plains. The white box denotes the region displayed in Fig. 4. (For interpretation of the references to color in this figure legend, the reader is referred to the web version of this article.)

material. Most regions within the southern highlands have crater morphological characteristics consistent with materials of yield strengths between that of wet soil and weak sedimentary rocks (but also consistent with highly fractured bedrock), whereas lowland craters are consistent with higher strength and less fractured crystalline rocks (Pike, 1980; Fig. 6).

Similar spatial trends are seen in surface thermophysical properties and the association of high thermal inertia crater surfaces with large depth to diameter ratios and complex crater onset diameters has been noted previously (Boyce et al., 2006; Tornabene et al., 2008). Nighttime THEMIS temperature data show this spatial correlation clearly through the presence of elevated nighttime temperatures associated with small (<5 km) diameter craters (Fig. 7). Immediately outside of these regions, such as southward from Utopia Planitia towards the transition to the southern highlands, small craters do not display elevated nighttime temperatures, indicating that competent, high-strength materials are largely absent or deeply buried. Regions with these distinctive thermophysical and crater morphological characteristics include Chryse, Acidalia, Utopia, and Isidis Planitias and Hesperia Planum (Figs. 8 and 9). The regions dominated by these high strength materials are all of Hesperian age or younger (Skinner et al., 2006). These observations indicate a crust dominated by poorly
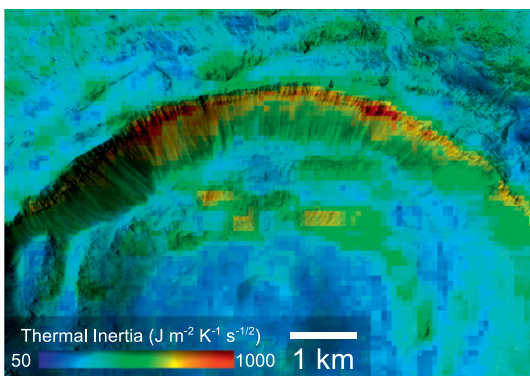

Fig. 6. Surface thermal inertia data within Chryse Planitia (near 318.4E, 27.1N) derived from 100 m/pixel THEMIS data (I07710001) with CTX image P21_009129_2073_XN_27N041W used for shading. High thermal inertia exposures are present within the crater walls, which are absent from many craters within older terrains.
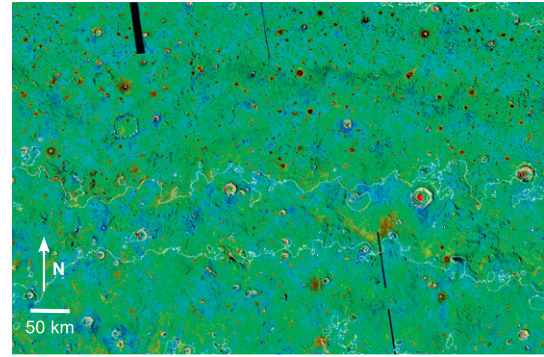

Fig. 7. THEMIS nighttime band 9 radiance global mosaic (color) overlaid on THEMIS daytime band 9 radiance global mosaic (shading). The image covers portions of Isidis Planitia and Utopia Planitia and is centered near 105E, 18N. Numerous small craters are present at lower elevations (top and left portions of the image) with high thermal inertia exposures (red and often darker shades). At the transition to the southern highlands (lower portion of the image), small craters become thermally indistinct from the surrounding terrain. White lines denote 500 m contours and elevation generally increases towards the south. (For interpretation of the references to color in this figure legend, the reader is referred to the web version of this article.)
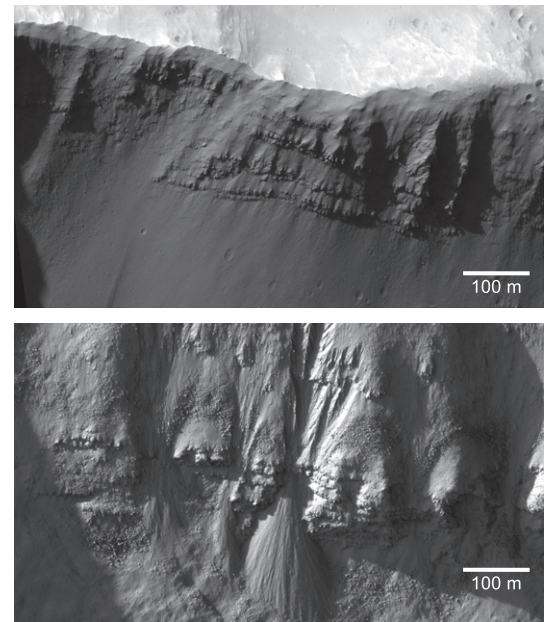

Fig. 8. Portions of HiRISE images ESP_017575_1590 (top) and PSP_009928_1600 (bottom). The two images show the contrast in materials exposed in well-preserved craters. The top image is near 139E, 21S in a region lacking high strength crustal materials. The bottom image is near 110E, 20S, within Hesperia Planum where younger surfaces display properties consistent with higher strength materials. There are clear exceptions to this pattern of materials exposed in crater walls, and pockets of blocky materials appear in fresh craters in older terrains. The solar incidence (for a level surface) is 67° in both images.

consolidated materials in older regions, while younger regions are dominated by higher strength rocks.

2.4. Observations at landing sites and martian meteorites

In situ observations can be used to characterize surface materials and, despite their limited areal coverage, provide additional insight into global orbital observations. The MER investigation within the Columbia Hills at Gusev Crater provides a close-up view of what may be an "island" of typical older highlands materials and
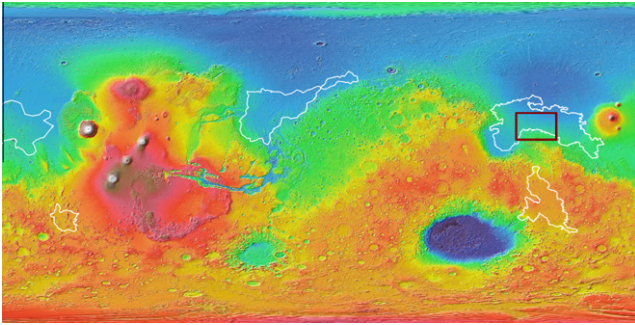
Fig. 9. White outlines show regions with relatively high thermal inertia craters similar to those shown in the northern portion of Fig. 7 (the background is the MOLA colorized shaded elevation map). Most regions are located within the northern lowlands at lower latitudes with the exception of Hesperia Planum and portions of Daedalia Plaunum. The area shown in Fig. 7 is denoted by the red box. (For interpretation of the references to color in this figure legend, the reader is referred to the web version of this article.)

stratigraphy in a region that was flooded by younger Hesperian lavas. A complex array of lithologies are present, but most consist of weakly consolidated clastic materials. These rocks have a lower thermal inertia than materials such as lava flows or volcanic blocks ($\sim$600 J m^{-2} K^{-1} s$^{-1/2}$; Fergason et al., 2006b) and are interpreted as ejecta and/or volcaniclastic materials that drape the local topography (Herkenhoff et al., 2006; McCoy et al., 2008). The rocks and outcrops present within the Columbia Hills have experienced a number of impact events (McCoy et al., 2008) and may be an example of structures typically present in the martian mega-regolith.

By contrast, high strength (with high thermal inertia values of 1200 J m^{-2} K^{-1} s$^{-1/2}$; Fergason et al., 2006b) solid basaltic blocks dominate the younger Gusev Plains. These materials have been linked to the high thermal inertia, high-olivine content rocky layers identified from orbit elsewhere (McSween et al., 2006; Bandfield and Rogers, 2008; Bandfield et al., 2011a). The Columbia Hills and the Gusev Plains may be representative of weakly consolidated ancient Noachian terrain and younger Hesperian effusive lavas respectively. Of course, it would be questionable to extrapolate with any confidence these properties planet-wide from a single site.

Outcrops of materials at the other MER landing site, Meridiani Planum, have elevated, but not extremely high thermal inertias and are somewhat cohesive (Fergason et al., 2006b; Okubo, 2007). Extensive layering is present throughout the region, but the materials are friable and none have thermal inertia values consistent with high strength blocks, such as would be the case with lavas or well-cemented sedimentary rocks (Fergason et al., 2006b). The lack of rocks in the plains of Meridiani Planum (most of the few rocks that have been identified are meteorites; Schröder et al., 2008) may indicate the lack of a regional strong, high inertia material, consistent with the lack of high thermal inertia surfaces detected in the region from orbit (Edwards et al., 2009). Boulders in this region are apparent immediately downslope of crater walls, as imaged by the Mars Exploration Rovers (MER), but are not cohesive enough to survive transport of distances greater than several hundred meters.

Rocks are abundant at both Viking and Pathfinder landing sites. Viking 2 is near both Mie Crater and Utopia Planitia (with apparent high crustal strength as discussed above). Both Viking 1 and Mars Pathfinder landing sites are close to regional near-surface high inertia units and ejecta from these units may dominate the rocks present at these sites.

At all of the landing sites discussed above, the presence or absence of rocks may be linked to the presence or absence of a regional high thermal inertia layer similar to that discussed in the previous section. Where this blocky, high thermal inertia layer is present, high resolution images show abundant blocks on the surface that are presumably derived from nearby craters that tap this layer (Fig. 10). An exception to this pattern can be seen at the Phoenix spacecraft landing site, where rocks are clearly present, but regional exposures of high thermal inertia bedrock are absent. The origin of the rocks as seen from orbit and the Phoenix landing site remains unclear and the potential effects of periglacial processes are unknown (Levy et al., 2009; Heet et al., 2009). Periglacial processes in general appear to have significant effects on the surface layer (e.g., Kreslavsky et al., 2008) and high thermal inertia bedrock surfaces are almost entirely absent at latitudes poleward of $\sim$45° (Edwards et al., 2009).

A similar set of circumstances may also apply to the martian meteorites, which may represent at least 7 and as many as 11 separate ejection events based on cosmic ray exposure ages (summarized in Nyquist et al. (2001)). With the exception of martian meteorite ALH84001 (older than 4 Ga), all existing meteorites are younger than $\sim$1.4 Ga (e.g., Hartmann and Neukum, 2001; Nyquist et al., 2001; McSween, 2008). Given the distribution of surface ages on Mars, it is remarkable that only a single sample out of more than 60 known martian meteorites to date formed during either the Noachian or Hesperian eras. The disparity in the age distribution of meteorites and martian surfaces has created some consternation and begs some explanation beyond a statistical anomaly.

Lunar meteorites, by contrast, sample a wide variety of lunar terrains, including lunar breccias (e.g., Korotev et al., 2009). The lack of variety in martian meteorites is consistent with a paucity of materials of older age that would survive ejection. For example, Hartmann and Neukum (2001) suggested that older terrains could be dominated by loosely cemented sediments that would not survive ejection at escape velocities. Given the evidence for impact breccias in the lunar meteorite collection, it seems that high strength rocks would survive ejection, even where they are present as products of highly disrupted bedrock.

3. Discussion

On Mars, competent bedrock and block-dominated surfaces are rare in older terrains. Less than 1% of the martian surface is composed of surfaces dominated by high strength rocks, and exposures of materials such as high strength blocky lava flows are extremely rare (Edwards et al., 2009; Fig. 11). In addition, extensive regions completely lack exposures of high strength rocks. Where we have the ability to probe the martian subsurface through craters, canyons, and other topographic features, THEMIS, CTX and HiRISE observations suggest that the older martian crust is typically mechanically weak and composed of weakly consolidated fine particulates. By contrast, younger terrains of Hesperian and Amazonian ages commonly show evidence for high strength crustal materials where subsequent dust mantling and periglacial processes have not occurred.

3.1. Potential interference from surface mantling

The clear contrast in both thermophysical and morphological properties distinguishes well-consolidated blocky materials from weakly consolidated and loose materials. However, mantling of surfaces by other materials may interfere with our assessment. In locations such as the high albedo and low thermal inertia surfaces of Tharsis, Elysium, and Arabia Terra, surfaces are likely to be pervasively mantled with aeolian dust (Kieffer et al., 1977; Christensen, 1986), which makes it difficult to assess the nature of the underlying materials. As a result, it is not clear what the physical nature of the crust is in these regions despite their extensive
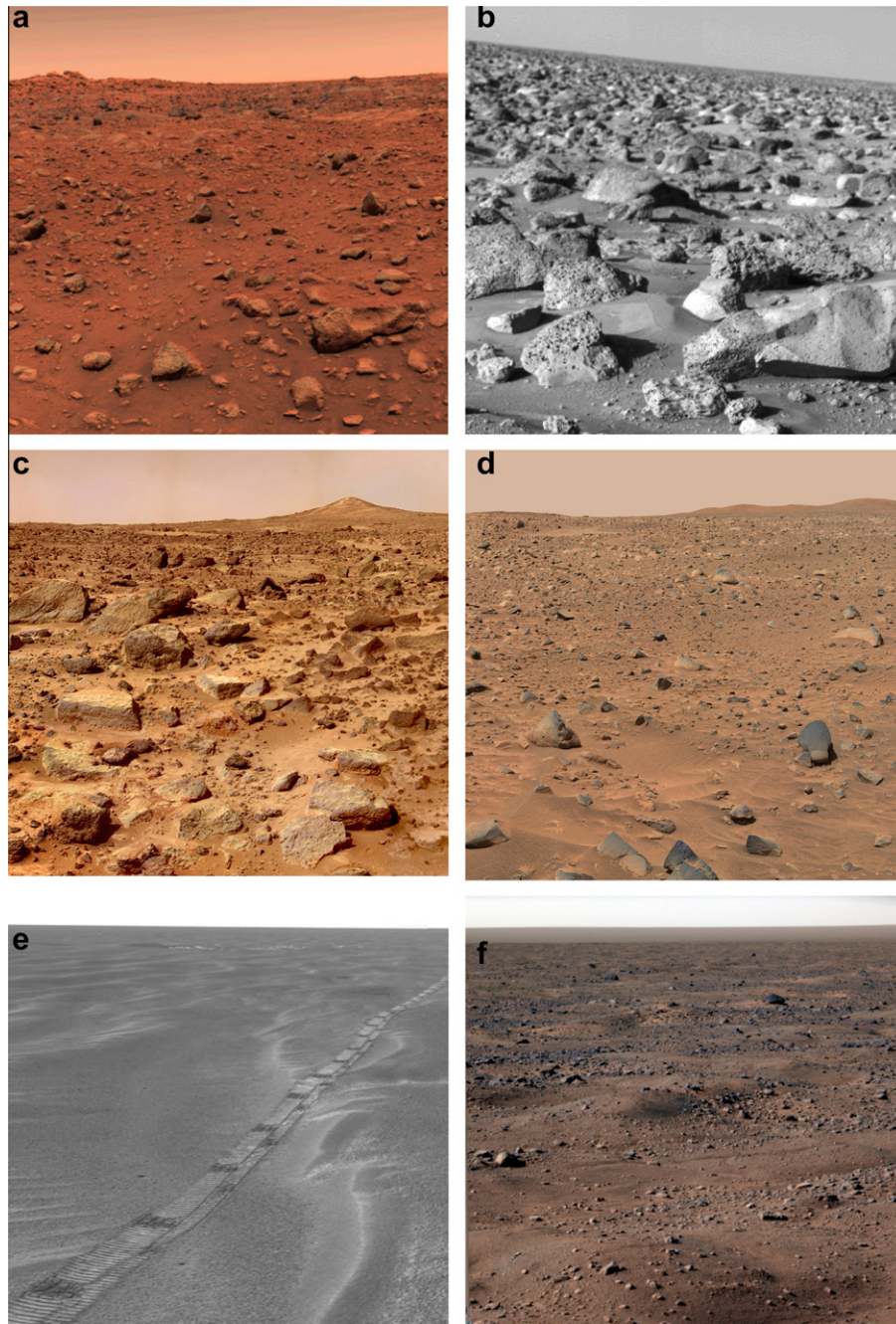
Fig. 10. Mars landing site images. (a) Viking 1; (b) Viking 2; (c) Mars Pathfinder; (d) MER-A; (e) MER-B; (f) Mars Scout Phoenix. Landing sites shown in images (a–d) all have high thermal inertia units present regionally. The MER-B landing side (Meridiani Planum) lacks both high strength rocks and regional high thermal inertia materials. The Mars Scout Phoenix landing site (68N, 233E) contains high strength rocks, but does not have a nearby high thermal inertia surface.

coverage. Based on the large-scale morphology of the Tharsis and Elysium volcanoes and Eastern Arabia Terra, both pyroclastic deposits and effusive lavas are present (e.g., Mouginis-Mark et al., 1988; Robbins et al., 2011; Fergason and Christensen, 2008).

Despite its common occurrence, the mantling surface cover is not ubiquitous and the physical nature of the underlying bedrock influences both the surface morphology and thermophysical properties in many regions. The canyon wall shown in Fig. 2 and the craters shown in Figs. 4–6 show clear examples of rocky materials immediately adjacent to poorly consolidated materials. There is no viable reason for aeolian mantling to occur on the steep crater walls but not the level crater floors. This suggests that the unconsolidated surface cover is derived locally from the easily disaggre-

gated underlying bedrock of the crater walls. The adjacent rocky crater floors show no such material and it is likely that the high strength materials do not degrade as significantly as the crater wall materials. In this case, the presence of the mantling material itself may add further support for the absence of high strength rocks on the crater walls. Although aeolian deposition and scouring may mantle some surfaces while keeping other surfaces clean, the spatial patterns present (e.g., radially symmetric exposures of bedrock isolated in crater floors entirely surrounded by poorly cohesive mantling materials) are not consistent with such a process.

There are many cases where surfaces of contrasting thermophysical properties are seen immediately adjacent to one another, including the walls of Valles Marineris and outflow channel walls
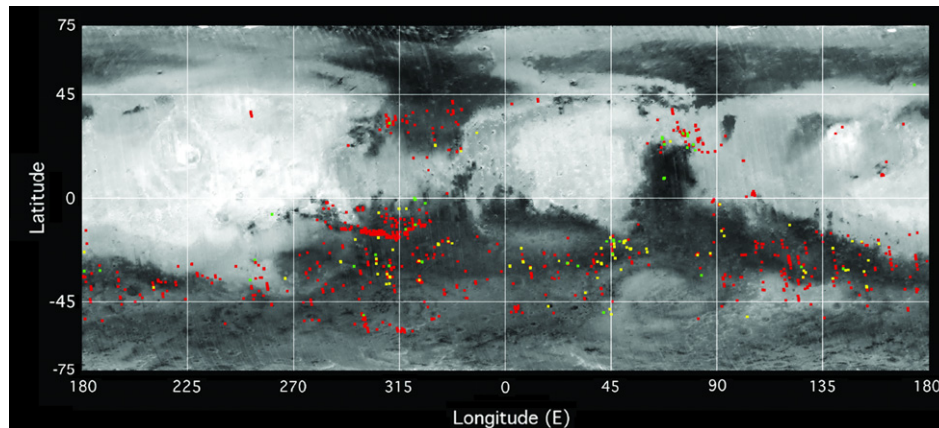
Fig. 11. Locations of high thermal inertia exposures consistent with the presence of surfaces dominated by high strength rocks (after Edwards et al. (2009)). Red points indicate crater and canyon wall locations, yellow points indicate crater floor locations, and green points indicate inter-crater plains locations. (For interpretation of the references to color in this figure legend, the reader is referred to the web version of this article.)

and floors where, once again, the channel floors are composed of high strength materials and walls are composed of poorly consolidated materials. These observations show that, with the exceptions of dust-mantled surfaces mentioned above, surface thermophysical properties typically reflect the properties of the underlying bedrock.

3.2. Comparison with other planetary bodies

3.2.1. Venus and the Moon

The lunar and venusian environments provide example surfaces for comparison to Mars. Although the Moon also contains a fine-particulate regolith, micrometeorite bombardment may be the source of much of this material. This process is not though to be pervasive on Mars due to its atmosphere and we might expect processes on the martian surface to be in some ways more like those of Venus.

In contrast to Mars, the bulk of the pervasively cratered lunar crust is derived from higher strength igneous rocks. The space weathering processes responsible for the creation of the fine particulate lunar regolith are thought to have been largely absent on the martian surface throughout its history. In the case of the Moon, younger craters expose blocky materials buried underneath the regolith, resulting in block-dominated crater floors, walls, and ejecta with high thermal inertias relative to the surrounding terrain (Bandfield et al., 2011b). An exception to this pattern of blocky lunar materials in young craters can be found in the lunar dark mantled deposits, which are thought to be composed of fine particulate explosive volcanic materials (e.g., Gaddis et al., 1985). In these regions, young craters do not expose blocky materials (Bandfield et al., 2011b).

As an example of a young, relatively pristine lunar crater, Giordano Bruno is a 22 km diameter crater on the lunar far side that shows extremely blocky surfaces despite the highly fractured lunar mega-regolith of the highlands terrain (Fig. 12). Crater counts indicate that this crater formed at 1–10 Ma (Morota et al., 2009) and has not been significantly degraded by micrometeorite bombardment. Both the floor and ejecta of the crater are dominated by blocky materials with Lunar Reconnaissance Orbiter Diviner Radiometer derived rock concentrations (which are sensitive mainly to rocks >1 m in diameter) that commonly reach 40% (Bandfield et al., 2011b). Although fine particulates can also be produced by impacts, they are poorly sorted and mixed with coarser materials. The mega-regolith of the Moon has both thermophysical and morphological properties that clearly indicate its blocky nature.
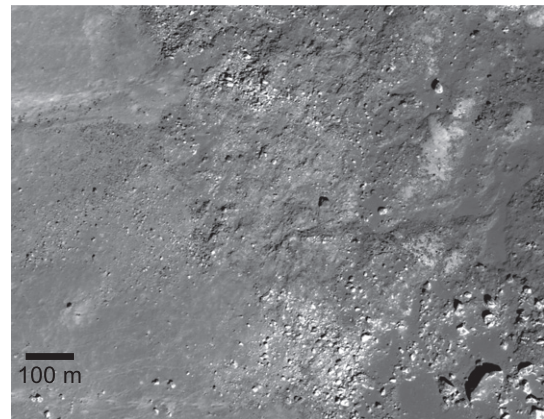

Fig. 12. Lunar Reconnaissance Orbiter Camera Image (M110919730; 35.9N, 102.6E) of the interior of Giordano Bruno, a young ~22 km diameter lunar impact crater. Lunar impacts produce abundant blocky materials (as well as impact melts) that are degraded over time by space weathering processes.

Venus may be an example of what to expect on the surface of a effusive lava-dominated planet without significant space or aqueous weathering processes. Images from the Venera landers show a surface that is broken and highly fractured, but still dominated by coarse gravel to large blocks (e.g., Gromov, 1998; Fig. 13). Despite the obvious and large differences between Venus and Mars surface environments, Venus may still be the best example of how we would expect the martian surface to appear in many regions if effusive lavas are prevalent.

3.2.2. Earth surfaces

Earth-based aerial imaging can provide a comparison to illustrate the contrast in materials observed at sub-meter scales comparable to the HiRISE images on Mars. For example, blocky basaltic lava flows in the Columbia River Basin show steep slopes, significant terracing, and abundant mass wasting of blocks at the base of slopes cut by floods during the late Pleistocene epoch (Fig. 14). Although the steep slopes and terracing may not be preserved in a mega-regolith, the formation of a mega-regolith in solid bedrock such as this would likely enhance the production of blocks.

Volcaniclastic deposits at Mount St. Helens, provide a clear contrast with the example of blocky materials from the Columbia River Basalts. Fig. 15 shows layered volcaniclastic deposits cut by

Fig. 13. Venera 14 lander image (YG06848) of the Venusian surface near 13S, 310E. Rocks dominate the landing sites and they persist in the venusian environment due to the lack of aqueous and space weathering processes.
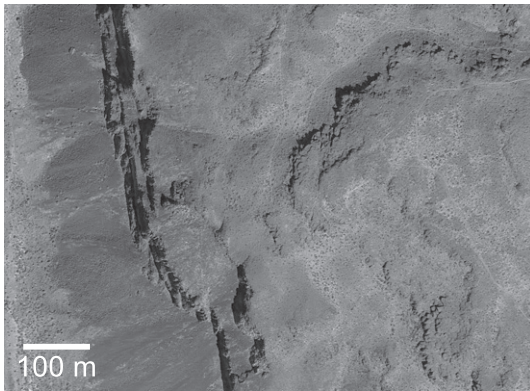

Image source Google Earth (Google 2012)

Fig. 14. Aerial orthoimage (near 46.9N, −120.0E) of Columbia River Basalts. Flows form stair step cliff and bench morphologies and dark toned surfaces at the base of cliffs are talus slopes composed of basalt blocks. Solar illumination is from the southeast.

a 150–200 m deep drainage along the western flank of the volcano. The talus slope that extends from the outcrop to the bottom of the drainage is dominated by fine-particulate material. The fine-grained, poorly consolidated nature of the slope is similar to surfaces on Mars where we suggest the outcrops are comprised of friable, volcaniclastic deposits. Most of the rare blocks present on the slope and at the base are likely from lithics entrained from the volcano during explosive eruptions. Similar to the martian examples, weakly consolidated blocks of pyroclastic materials are also present, but they break apart downslope and do not collect at the base of the canyon.
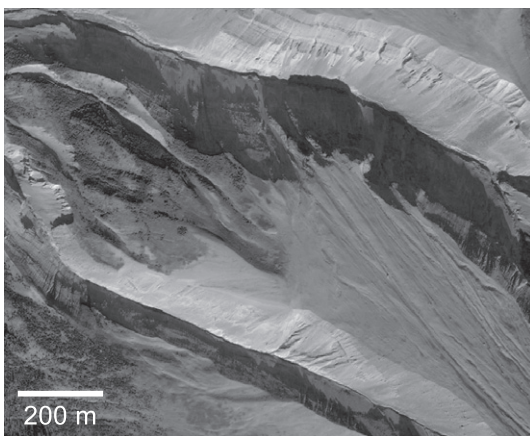

Image source Google Earth (Google 2012, DigitalGlobe 2012)

Fig. 15. Aerial orthoimage (near 46.2N, −122.2E) of incised pyroclastic deposits from Mount Saint Helens. Incised surfaces and their base are largely free of blocks. Active downcutting has occurred rapidly and fluvial erosion produces fine particulate materials that are easily washed downstream. Solar illumination is from the south.

Where high strength rocks are present in arid, vegetation-free environments on Earth, they are associated with steep slopes such as canyon walls and commonly have talus slopes that form at the base and persist for extended periods of time. These features are detected only in isolated locations within older martian terrain and should be much more pervasive if high-strength blocky materials were dominant.

3.3. Explosive volcanism as a potential source

If the upper crustal materials are not dominated by lava flows or other high strength materials, what is the origin of the martian upper crust? Based on their strength, thermal inertia, and morphological characteristics, typical older crustal materials consist of fine-particulates (sand and smaller particle sizes) that are weakly indurated, sometimes with numerous rhythmic stratigraphic sequences. These deposits are generally unaltered or lightly altered and basaltic in composition (e.g., Edgett and Lancaster, 1993; Bandfield et al., 2000; Mustard et al., 2005). Basaltic volcaniclastics, primary or reworked, are good candidate materials for the origin of much of the older Noachian crust.

Certainly aeolian and aqueous clastic deposits may be present as well. For example, layered deposits are present within Meridiani Planum that appear to be due to a combination of aqueous and aeolian processes (Grotzinger et al., 2005). These materials have unique morphological and compositional properties and likely have a different origin than the bulk of the highlands crust. Despite these exceptions, we might consider Mars a planet dominated by volcanic ash rather than lava flows, and suggest that explosive volcanism likely played a prominent role in the development of the upper martian crust.

Indeed, the products of explosive volcanism have long been identified on the surface of Mars (e.g., Carr, 1973; Greeley and Spudis, 1981; Scott and Tanaka, 1982; Mouginis-Mark et al., 1988; Wilson and Head, 1994; Edgett, 1997; Squyres et al., 2007), and are thought to have been more common during early martian history (e.g., West, 1974; Reimers and Komar, 1979; Mouginis-Mark et al., 1988). These observations are also consistent with interpretations of large ash flow sheets and tehpra identified in isolated regions (e.g., Wilson and Head, 1994; Mandt et al., 2008; Crown and Greeley, 1993).

A transition from explosive to effusive volcanism is supported by several recent studies. Kerber and Head (2010) performed a stratigraphic analysis of the Medusae Fossae Formation (MFF), an extensive deposit (estimated at 1.4×10^6 km^3; Bradley et al., 2002) that has been suggested to have an explosive volcanic source (though aeolian dust is an alternate source and at least some of the deposits have undergone aeolian reworking). As also indicated by Zimberlman and Scheidt (2012), the MFF appears to be much older than previously realized and in many cases the deposits are embayed by Hesperian lavas, suggesting that the MFF predates a transition to effusive volcanism.

Robbins et al. (2011) analyzed the ages of deposits from 20 martian volcanoes and identified a change around 3.2–3.5 Ga from

explosive to more effusive eruption styles associated with martian volcanic constructs during the Hesperian Era. The development of Alba Mons has been shown in particular to bridge this transition from explosive to effusive activity (Mouginis-Mark et al., 1988; Ivanov and Head, 2006) and the changing eruption style of martian volcanoes from explosive to effusive is not a new idea (e.g., Reimers and Komar, 1979). Our results suggest that explosive volcanism not only occurred, but may have been pervasive over much of early martian history, leaving a lasting signature in the composition of the martian crust.

This transition has been attributed to the drying out of a permafrost-rich upper crust (Reimers and Komar, 1979). The interaction of magma and water creates both the means to produce explosive volcanic activity as well as a heat source to melt ice and mobilize water. In a rough sense, the presence of both water and volcanic activity on Mars may be both responsible for the explosive activity as well as providing an aqueous source for the production of phyllosilicates and other altered materials in the subsurface (Barnhart et al., 2010; Tosca and Hurowitz, 2011; Ehlmann et al., 2011).

Although groundwater is a potential source for high volatile content volcanic eruptions, high juvenile volatile contents may also be responsible for a significant transfer of water and CO_2 from the interior to the surface and atmosphere of Mars (Mouginis-Mark et al., 1982). The switch to more effusive volcanism during the Hesperian and Amazonian eras would have reduced the influence of global volcanism on the martian atmosphere and climate and perhaps may indicate a reduction in the volatile content of the mantle.

A potential issue for this hypothesis is the lack of clearly identifiable source vents for the enormous volumes of volcaniclastic materials. As an example, it has been proposed that Apollinaris Patera may be the source of the MFF (Kerber et al., 2011). It is not clear, however, if it is realistic for a volcanic construct to explosively produce a deposit much larger in volume than the construct itself (Zimbelman, personal communication). Regardless of the process, these materials must have an origin of some sort, which remains unknown.

3.4. Fluvial erosion

Regardless of the source of the materials, their physical properties have a large influence on subsequent development of the crust. Layers of high strength materials interspersed with the more typically weak crustal materials display a clear contrast in their relative ease of erosion. For example, terrestrial bedrock incision rates can vary by at least five orders of magnitude based on the resistance of the lithology (Stock and Montgomery, 1999). Outflow channels, such as Kasei and Ares Valles have weak, poorly consolidated walls with floors of stronger high thermal inertia materials. The high thermal inertia floors are spatially, but not stratigraphically, extensive. It is likely that outflow floods easily and extensively carved through the weak crustal materials, but were often controlled by the presence of high-strength materials, which may have enhanced lateral erosion and prevented further downcutting.

Poorly consolidated fine-particulate materials are easy to erode and transport and estimates of water volumes necessary to create large channel features on Mars are likely too high unless they explicitly consider this situation. This would indicate water volumes that are likely at the lower end of the range of discharge estimates in previous studies (e.g., Howard et al., 2005; Leask et al., 2007).

The presence of weakly consolidated, fine-grained materials also has implications for the formation of groundwater sapping channels on Mars. Based on analogous morphologies present in Hawaii and the Colorado Plateau, the formation of simple channels (such as Nirgal Valles) on Mars have been often considered to be formed as a result of headward erosion (e.g., Laity and Malin, 1985). This formation process has been called into question recently based largely on the difficulty of sapping processes to effectively erode, break down, and transport high-strength bedrock materials (Lamb et al., 2006; Luo and Howard, 2008). For example, even in a poorly cohesive material, fine particulates will be transported away, leaving a coarse-particulate lag deposit that will effectively shut off further headward erosion (Lamb et al., 2006). Although the process forming these channels remains ambiguous, it appears that crustal materials composed of poorly cohesive fine-particulates would allow for groundwater sapping to remain a viable formation mechanism for carving some martian channels.

4. Conclusions and implications

The dual nature of the crust appears to be a defining characteristic of martian history. How can the upper martian crust be accurately described in terms of its basic makeup? There is evidence for the presence of a mega-regolith, lava flows, and extensive layers of aeolian, fluvial, or volcaniclastic sediments. Where we have the ability to probe the martian subsurface through craters, canyons, and other topographic features, the older martian crust is typically mechanically weak and dominated by poorly consolidated fine particulates while younger materials are dominated by high strength blocks that may be composed of effusive lavas. The presence of isolated layers of high strength rock in older regions clearly show exceptions to this general pattern, however.

In older Noachian terrains, both crater and valley wall morphologies and thermal inertia measurements are typically consistent with a crust composed of poorly consolidated fine-particulate material. Surface mantling via aeolian processes may be invoked in some cases to hide high strength rock. The positive identification of competent rock in both isolated areas and younger regions lends confidence to the interpretation of a lack of high strength rock or blocky materials in immediately adjacent surfaces and elsewhere.

The imaging and thermophysical measurements are supported by other observations. The presence or absence of rocks in the terrain at various landing sites can be explained by the presence or absence of a local high thermal inertia unit. The lack of high strength rocks in older terrain would also explain the anomalously young ages of the martian meteorites relative to the global distribution of surface ages. Finally, surface slopes and crater morphologies investigated by others are also consistent with an older crust composed of poorly cohesive materials, which (based on morphological and thermophysical properties) cannot be dominated by high strength blocky materials even if they are highly fractured.

Volcaniclastic materials in older terrains, reworked or otherwise, are good candidate materials consistent with these observations. Although alternate sources of the crustal materials are possible, early Mars appears to have been a volcaniclastic planet dominated by explosive volcanism that later transitioned to more effusive styles of eruptions during the Hesperian era. This represents a style of development and evolution that is unique from the other terrestrial planets, and has implications both to the evolution of the crust and mantle as well as the development of the surface morphology, including fluvial channel development. Although there are clearly exceptions (e.g., the laterally extensive lava flows near the base of Valles Marineris), the general correlation of the weak nature of the crustal materials with older regions of Mars suggests a dramatic change in the style of volcanism with time.

teams for their efforts in producing excellent datasets and observations used here. Jim Zimbelman and an anonymous reviewer provided thoughtful and constructive comments that both improved and clarified the manuscript. Thanks also to Phil Christensen and Nick Tosca for supportive arguments and discussions. JMARS software, developed at Arizona State University, was used for much of the data analysis and construction of figures presented here.

References

Adams, J.B. et al., 2009. Salt tectonics and collapse of Hebes Chasma, Valles Marineris, Mars. Geology 37 (8), 691–694.

Bandfield, J.L., Rogers, A.D., 2008. Olivine dissolution by acidic fluids in Argyre Planitia, Mars: Evidence for a widespread process? Geology 36. http://dx.doi.org/10.1130/G24724A.1.

Bandfield, J.L., Hamilton, V.E., Christensen, P.R., 2000. A global view of martian surface compositions from MGS-TES. Science 287, 1626–1630. http://dx.doi.org/10.1126/science.287.5458.1626.

Bandfield, J.L., Rogers, A.D., Edwards, C.S., 2011a. The role of aqueous alteration in the formation of martian soils. Icarus. http://dx.doi.org/10.1016/j.icarus.2010.08.028.

Bandfield, J.L., Ghent, R.R., Vasavada, A.R., Paige, D.A., Lawrence, S.J., Robinson, M.S., 2011b. Lunar surface rock abundance and regolith fines temperatures derived from LRO Diviner Radiometer data. J. Geophys. Res. 116. http://dx.doi.org/10.1029/2011JE003866.

Barnhart, C.J., Nimmo, F., Travis, B.J., 2010. Martian post-impact hydrothermal systems incorporating freezing. Icarus 208, 101–117. http://dx.doi.org/10.1016/j.icarus.2010.01.013.

Beyer, R.A., McEwen, A.S., 2005. Layering stratigraphy of eastern Coprates and northern Capri Chasmata, Mars. Icarus 179, 1–23. http://dx.doi.org/10.1016/j.icarus.2005.06.014.

Boyce, J.M., Mouginis-Mark, P., Garbeil, H., Tornabene, L.L., 2006. Deep impact craters in the Isidis and southwestern Utopia Planitia regions of Mars: High target material strength as a possible cause. Geophys. Res. Lett. 33, 6202. http://dx.doi.org/10.1029/2005GL024462.

Bradley, B.A., Sakimoto, S.E.H., Frey, H., Zimbelman, J.R., 2002. Medusae Fossae Formation: New perspectives from Mars Global Surveyor. J. Geophys. Res. 107, 5058. http://dx.doi.org/10.1029/2001JE001537.

Carr, M.H., 1973. Volcanism on Mars. J. Geophys. Res. 78, 4049–4062. http://dx.doi.org/10.1029/JB078i020p04049.

Caruso, P.A., Schultz, R.A., 2001. Slope stability and lithology for interior layered deposits and wallrock in Valles Marineris. Lunar Planet. Sci. Conf. 32, 1745.

Christensen, P.R., 1986. Regional dust deposits on Mars: Physical properties, age, and history. J. Geophys. Res. 91, 3533–3545.

Christensen, P.R. et al., 2004. The Thermal Emission Imaging System (THEMIS) for the Mars 2001 Odyssey Mission. Space Sci. Rev. 110, 85–130. http://dx.doi.org/10.1023/B:SPAC.0000021008.16305.94.

Clow, G.D., Moore, H.J., Davis, P.A., Strichartz, L.R., 1988. Stability of Chasma Walls in the Valles Marineris, Mars. Lunar Planet. Sci. Conf. 19, 201.

Crown, D.A., Greeley, R., 1993. Volcanic geology of Hadriaca Patera and the eastern Hellas region of Mars. J. Geophys. Res. 98, 3431–3451. http://dx.doi.org/10.1029/92JE02804.

Edgett, K.S., 1997. Aeolian dunes as evidence for explosive volcanism in the Tharsis region of Mars. Icarus 130, 96–114. http://dx.doi.org/10.1006/icar.1997.5806.

Edgett, K.S., Lancaster, N., 1993. Volcaniclastic aeolian dunes. J. Arid Environ. 25, 271–297.

Edwards, C.S., Christensen, P.R., Hamilton, V.E., 2008. Evidence for extensive olivine-rich basalt bedrock outcrops on Ganges and Eos chasmas, Mars. J. Geophys. Res. 113, 11003. http://dx.doi.org/10.1029/2008JE003091.

Edwards, C.S., Bandfield, J.L., Christensen, P.R., Fergason, R.L., 2009. Global distribution of bedrock exposures on Mars using THEMIS high-resolution thermal inertia. J. Geophys. Res. 114, 11001. http://dx.doi.org/10.1029/2009JE003363.

Edwards, C.S., Nowicki, K.J., Christensen, P.R., Hill, J., Gorelick, N., Murray, K., 2011. Mosaicking of global planetary image datasets: 1. Techniques and data processing for Thermal Emission Imaging System (THEMIS) multi-spectral data. J. Geophys. Res. 116. http://dx.doi.org/10.1029/2010JE003755.

Ehlmann, B.L. et al., 2011. Subsurface water and clay mineral formation during the early history of Mars. Nature 479, 53–60. http://dx.doi.org/10.1038/nature10582.

Fergason, R.L., Christensen, P.R., 2008. Formation and erosion of layered materials: Geologic and dust cycle history of Eastern Arabia Terra Mars. J. Geophys. Res. 113. http://dx.doi.org/10.1029/2007JE002973.

Fergason, R.L., Christensen, P.R., Kieffer, H.H., 2006a. High-resolution thermal inertia derived from the Thermal Emission Imaging System (THEMIS): Thermal model and applications. J. Geophys. Res. 111, 12004. http://dx.doi.org/10.1029/2006JE002735.

Fergason, R.L., Christensen, P.R., Bell, J.F., Golombek, M.P., Herkenhoff, K.E., Kieffer, H.H., 2006b. Physical properties of the Mars Exploration Rover landing sites as inferred from Mini-TES-derived thermal inertia. J. Geophys. Res. 111, 2. http://dx.doi.org/10.1029/2005JE002583.

Gaddis, L.R., Pieters, C.M., Hawke, B.R., 1985. Remote sensing of lunar pyroclastic mantling deposits. Icarus 61, 461–489. http://dx.doi.org/10.1016/0019-1035(85), 90136-8.

Greeley, R., Spudis, P.D., 1981. Volcanism on Mars. Rev. Geophys. Space Phys. 19, 13–41. http://dx.doi.org/10.1029/RG019i001p00013.

Gromov, V., 1998. Physical and mechanical properties of lunar and planetary soils. Earth, Moon, Planets 80, 51–72. http://dx.doi.org/10.1023/A:1006353510204.

Grotzinger, J.P. et al., 2005. Stratigraphy and sedimentology of a dry to wet eolian depositional system, Burns formation, Meridiani Planum, Mars. Earth Planet. Sci. Lett. 240. http://dx.doi.org/10.1016/j.epsl.2005.09.039.

Hartmann, W.K., Neukum, G., 2001. Cratering chronology and the evolution of Mars. Space Sci. Rev. 96, 165–194.

Heet, T.L., Arvidson, R.E., Cull, S.C., Mellon, M.T., Seelos, K.D., 2009. Geomorphic and geologic settings of the Phoenix Lander mission landing site. J. Geophys. Res. 114. http://dx.doi.org/10.1029/2009JE003416.

Herkenhoff, K.E. et al., 2006. Overview of the Microscopic Imager Investigation during Spirit's first 450 sols in Gusev Crater. J. Geophys. Res. 111, 2. http://dx.doi.org/10.1029/2005JE002574.

Howard, A.D., Moore, J.M., Irwin, R.P., 2005. An intense terminal epoch of widespread fluvial activity on early Mars: 1. Valley network incision and associated deposits. J. Geophys. Res. 110, 12. http://dx.doi.org/10.1029/2005JE002459.

Ivanov, M.A., Head, J.W., 2006. Alba Patera, Mars: Topography, structure, and evolution of a unique late Hesperian–early Amazonian shield volcano. J. Geophys. Res. 111, 9003. http://dx.doi.org/10.1029/2005JE002469.

Jackson, M.P.A., Adams, J.B., Dooley, T.P., Gillespie, A.R., Montgomery, D.R., 2011. Modeling the collapse of Hebes Chasma, Valles Marineris, Mars. Geol. Soc. Am. Bull. 123. http://dx.doi.org/10.1130/B30307.1.

Kerber, L., Head, J.W., 2010. The age of the Medusae Fossae Formation: Evidence of Hesperian emplacement from crater morphology, stratigraphy, and ancient lava contacts. Icarus 206, 669–684. http://dx.doi.org/10.1016/j.icarus.2009.10.001.

Kerber, L., Head, J.W., Madaleine, J.-B., Forget, F., Wilson, L., 2011. The dispersal of pyroclasts from Apollinaris Patera, Mars: Implications for the origin of the Medusae Fossae Formation. Icarus 216. http://dx.doi.org/10.1016/j.icarus.2011.07.035.

Kieffer, H.H., Martin, T.Z., Peterfreund, A.R., Jakosky, B.M., Miner, E.D., Palluconi, F.D., 1977. Thermal and albedo mapping of Mars during the Viking primary mission. J. Geophys. Res. 82, 4249–4291. http://dx.doi.org/10.1029/JS082i028p04249.

Korotev, R.L., Zeigler, R.A., Jolliff, B.L., 2009. Compositional and lithological diversity among brecciated lunar meteorites of intermediate iron concentration. Meteorit. Planet. Sci. 1322, 1287–1322.

Kreslavsky, M.A., Head, J.W., Marchant, D.R., 2008. Periods of active permafrost layer formation during the geological history of Mars: Implications for circum-polar and mid-latitude surface processes. Planet. Space Sci. 56, 289–302. http://dx.doi.org/10.1016/j.pss.2006.02.010.

Laity, J.E., Malin, M.C., 1985. Sapping processes and the development of theater-headed valley networks on the Colorado Plateau. GSA Bull. 96, 203–217.

Lamb, M.P., Howard, A.D., Johnson, J., Whipple, K.X., Dietrich, W.E., Perron, J.T., 2006. Can springs cut canyons into rock? J. Geophys. Res. 111, 7002. http://dx.doi.org/10.1029/2005JE002663.

Leask, H.J., Wilson, L., Mitchell, K.L., 2007. Formation of Mangala Valles outflow channel, Mars: Morphological development and water discharge and duration estimates. J. Geophys. Res. 112, 8003. http://dx.doi.org/10.1029/2006JE002851.

Levy, J.S., Head, J.W., Marchant, D.R., 2009. Cold and dry processes in the martian arctic: Geomorphic observations at the Phoenix landing site and comparisons with terrestrial cold desert landforms. Geophys. Res. Lett. 36, 21203. http://dx.doi.org/10.1029/2009GL040634.

Lucchitta, B.K. et al., 1992. The canyon system on Mars. In: Kieffer, H.H. et al. (Ed.), Mars, pp. 453–492.

Luo, W., Howard, A.D., 2008. Computer simulation of the role of groundwater seepage in forming martian valley networks. J. Geophys. Res. 113, 5002. http://dx.doi.org/10.1029/2007JE002981.

Malin, M.C., Edgett, K.S., 2000. Sedimentary rocks of early Mars. Science 290, 1927–1937. http://dx.doi.org/10.1126/science.290.5498.

Malin, M.C. et al., 2007. Context Camera Investigation on board the Mars Reconnaissance Orbiter. J. Geophys. Res. 112, 5. http://dx.doi.org/10.1029/2006JE002808.

Mandt, K.E., de Silva, S.L., Zimbelman, J.R., Crown, D.A., 2008. Origin of the Medusae Fossae Formation, Mars: Insights from a synoptic approach. J. Geophys. Res. 113, 12011. http://dx.doi.org/10.1029/2008JE003076.

McCoy, T.J. et al., 2008. Structure, stratigraphy, and origin of Husband Hill, Columbia Hills, Gusev Crater, Mars. J. Geophys. Res. 113, 6. http://dx.doi.org/10.1029/2007JE003041.

McEwen, A.S., Malin, M.C., Carr, M.H., Hartmann, W.K., 1999. Voluminous volcanism on early Mars revealed in Valles Marineris. Nature 397, 584–586. http://dx.doi.org/10.1038/17539.

McEwen, A.S. et al., 2007. Mars Reconnaissance Orbiter's High Resolution Imaging Science Experiment (HiRISE). J. Geophys. Res. 112. http://dx.doi.org/10.1029/2005JE002605.

McSween Jr., H.Y., 2008. Martian meteorites as crustal samples. In: Bell, J.F. (Ed.), The Martian Surface: Composition, Mineralogy, and Physical Properties. Cambridge University Press, pp. 383–395.

McSween Jr., H.Y. et al., 2006. Characterization and petrologic interpretation of olivine-rich basalts at Gusev Crater, Mars. J. Geophys. Res. 111, 2. http://dx.doi.org/10.1029/2005JE002477.

Mellon, M.T., Jakosky, B.M., Kieffer, H.H., Christensen, P.R., 2000. High-resolution thermal inertia mapping from the Mars Global Surveyor Thermal Emission Spectrometer. Icarus 148, 437–455. http://dx.doi.org/10.1006/icar.2000.6503.

Morota, T. et al., 2009. Formation age of the lunar crater Giordano Bruno. Meteorit. Planet. Sci. 44. http://dx.doi.org/10.1111/j.1945-5100.2009.tb01211.x.

Mouginis-Mark, P.J., Head III, J.W., Wilson, L., 1982. Explosive volcanism on Hecates Tholus, Mars – Investigation of eruption conditions. J. Geophys. Res. 87, 9890–9904. http://dx.doi.org/10.1029/JB087iB12p09890.

Mouginis-Mark, P.J., Wilson, L., Zimbelman, J.R., 1988. Polygenic eruptions on Alba Patera, Mars. Bull. Volcanol. 50, 361–379. http://dx.doi.org/10.1007/BF01050636.

Mustard, J.F. et al., 2005. Olivine and pyroxene diversity in the crust of Mars. Science 307, 1594–1597. http://dx.doi.org/10.1126/science.1109098.

Nyquist, L.E., Bogard, D.D., Shih, C.-Y., Greshake, A., Stoumlffler, D., Eugster, O., 2001. Ages and geologic histories of martian meteorites. Space Sci. Rev. 96, 105–164.

Okubo, C.H., 2007. Strength and deformability of light-toned layered deposits observed by MER Opportunity: Eagle to Erebus craters, Mars. Geophys. Res. Lett. 34, 20205. http://dx.doi.org/10.1029/2007GL031327.

Peulvast, J., 2001. Morphology, evolution and tectonics of Valles Marineris wallslopes (Mars). Geomorphology 37, 329–352. http://dx.doi.org/10.1016/S0169-555X(00), 00085-4.

Pike, R.J., 1980. Control of crater morphology by gravity and target type – Mars, Earth, Moon. Lunar Planet. Sci. Conf. 11, 2159–2189.

Piqueux, S., Christensen, P.R., 2011. Temperature-dependent thermal inertia of homogeneous martian regolith. J. Geophys. Res. 116, 7004. http://dx.doi.org/10.1029/2011JE003805.

Presley, M.A., Christensen, P.R., 1997. The effect of bulk density and particle size sorting on the thermal conductivity of particulate materials under martian atmospheric pressures. J. Geophys. Res. 102, 9221–9230. http://dx.doi.org/10.1029/97JE00271.

Reimers, C.E., Komar, P.D., 1979. Evidence for explosive volcanic density currents on certain martian volcanoes. Icarus 39, 88–110. http://dx.doi.org/10.1016/0019-1035(79), 90103-9.

Robbins, S.J., Achille, G.D., Hynek, B.M., 2011. The volcanic history of Mars: High-resolution crater-based studies of the calderas of 20 volcanoes. Icarus 211, 1179–1203. http://dx.doi.org/10.1016/j.icarus.2010.11.012.

Rogers, A.D., Christensen, P.R., Bandfield, J.L., 2005. Compositional heterogeneity of the ancient martian crust: Analysis of Ares Vallis bedrock with THEMIS and TES data. J. Geophys. Res. 110, 5010. http://dx.doi.org/10.1029/2005JE002399.

Schröder, C. et al., 2008. Properties and distribution of paired candidate stony meteorites at Meridiani Planum, Mars, J. Geophys. Res. 115. http://dx.doi.org/10.1029/2010JE003616.

Schultz, R.A., 1991. Structural development of Coprates Chasma and western Ophir Planum, Valles Marineris Rift, Mars. J. Geophys. Res. 96, 22777. http://dx.doi.org/10.1029/91JE02556.

Schultz, R.A., 1996. Fault-length statistics and implications of graben sets at Candor Mensa, Mars. J. Struct. Geol. 18, 373–383. http://dx.doi.org/10.1016/S0191-8141(96), 80057-5.

Schultz, R.A., 2002. Stability of rock slopes in Valles Marineris, Mars. Geophys. Res. Lett. 29, 190000-1. http://dx.doi.org/10.1029/2002GL015728.

Scott, D.H., Tanaka, K.L., 1982. Ignimbrites of Amazonis Planitia region of Mars. J. Geophys. Res. 87, 1179–1190. http://dx.doi.org/10.1029/JB087iB02p01179.

Skinner Jr., J.A., Hare, T.M., Tanaka, K.L., 2006. Digital renovation of the atlas of Mars 1:15,000,000-scale global geologic series maps. Lunar Planet. Sci. Conf. 37, 2331.

Squyres, S.W. et al., 2007. Pyroclastic activity at home plate in Gusev Crater, Mars. Science 316, 738. http://dx.doi.org/10.1126/science.1139045.

Stewart, S.T., Valiant, G.J., 2006. Martian subsurface properties and crater formation processes inferred from fresh impact crater geometries. Meteorit. Planet. Sci. 41, 1509–1537.

Stock, J.D., Montgomery, D.R., 1999. Geologic constraints on bedrock river incision using the stream power law. J. Geophys. Res. 104, 4983–4994. http://dx.doi.org/10.1029/98JB02139.

Tornabene, L.L., Moersch, J.E., McSween, H.Y., Hamilton, V.E., Piatek, J.L., Christensen, P.R., 2008. Surface and crater-exposed lithologic units of the Isidis Basin as mapped by coanalysis of THEMIS and TES derived data products. J. Geophys. Res. 113, 10001. http://dx.doi.org/10.1029/2007JE002988.

Tosca, N.J., Hurowitz, J.A., 2011. Neoformation, diagenesis and the clay cycle on early Mars. Lunar Planet. Sci. Conf. 42, 2031.

West, M., 1974. Martian volcanism: Additional observations and evidence for pyroclastic activity. Icarus 21, 1. http://dx.doi.org/10.1016/0019-1035(74)90085-2.

Wilson, L., Head III, J.W., 1994. Mars: Review and analysis of volcanic eruption theory and relationships to observed landforms. Rev. Geophys. 32, 221–263. http://dx.doi.org/10.1029/94RG01113.